2024 IEEE Ultrasonics, Ferroelectrics, and Frequency Control Joint Symposium (UFFC-JS) | 979-8-3503-7190-1/24/$31.00 ©2024 IEEE | DOI: 10.1109/UFFC-JS60046.2024.10793946

A Millimeter Wave Ferroelectric Hafnium Zirconium Oxide-based Programmable Antenna

Samuel Quaresima*, Nicolas Casilli*, Vitaly Petrov†, Josep Miquel Jornet‡,
Luca Colombo*, Benyamin Davaji*, Cristian Cassella*

*Institute for NanoSystems Innovation (NanoSI), Northeastern University, Boston, MA, USA
†Division of Communication Systems (CoS), KTH Royal Institute of Technology, Stockholm, SWE
‡Institute for the Wireless Internet of Things (WIoT), Northeastern University, Boston, MA, USA

***Abstract*—In this work, we present an on-chip Hafnium Zirconium Oxide-based millimeter wave (mmWave) programmable antenna. The device exhibits a resonance frequency of 36.623 GHz, which can be programmed by varying the polarization state of a thin Hafnium Zirconium Oxide (HZO) layer enclosed in the structure of the antenna. By polarizing such HZO film, we demonstrate, for the first time, a variation in the resonance frequency for ferroelectrically programmable antennas without continuously applying a bias. In this regard, the non-volatile behavior of HZO allows to retain the polarization state of the film even after removing the DC voltage, therefore enabling the antenna's resonance frequency retention. The full ferroelectric switching of the HZO layer occurs approximately at ±3 V, resulting in a maximum resonance frequency shift of 3.019 GHz (8.3% fractional frequency change) between different programming voltages. The device's response to the applied programming voltage generates a ferroelectrically-induced hysteresis on its resonance frequency. In contrast to prior devices of this class, the proposed approach showcases a more compact size, full post-CMOS compatibility, low programming voltage, and non-volatile programmability.**

***Index Terms*—Ferroelectric Devices, Reconfigurable Antennas, Ultrawideband Antennas, Hafnium Alloys.**

I. Introduction

Driven by the increasing need for frequency agility in fifth-generation (5G) communication systems and by the approaching sixth-generation (6G) era, designers of wireless front-ends are facing growing challenges to increase the data rates exploitable for communication while preserving low power consumption [1]. Equipping radiofrequency front-ends (RFFEs) with programmable components is an effective approach to enable improved power efficiencies through adaptive reconfiguration based on instantaneous power and communication requirements [2]. The development of reconfigurable on-chip antennas is particularly important as it can lead to the optimization of transceivers power efficiencies and throughput regardless of the active operating mode of power amplifiers (PAs) [3]. Similarly, developing these antennas would allow us to reduce any self-interference coming from the impedance mismatch between PAs' output impedance and antennas' input impedance [4].

This work has been supported by the U.S. Air Force Office of Scientific Research (AFOSR), award FA9550-23-1-0254.
e-mail: c.cassella@northeastern.edu, quaresima.s@northeastern.edu

Different methods combining antennas with micro-electromechanical systems (MEMS) [5], graphene [6], phase-change materials [7] or metamaterials [8] have been recently proposed to achieve programmable antennas. However, the non-compact form factor, the high direct current (DC) voltage required, and the challenging fabrication requirements make these existing methods hard to exploit, especially when adopting circuital elements manufactured using established complementary metal-oxide-semiconductor (CMOS) fabrication techniques [9].

The use of ferroelectric components to program antennas' response has been recently explored [10]–[12], with $(\mathrm{KTa}_x, \mathrm{Nb}_{1-x})\mathrm{O}_3$ (KTN) [13], $(\mathrm{K}_{0.5}, \mathrm{Na}_{0.5})\mathrm{NbO}_3$ (KNN) [14] and $(\mathrm{Ba}, \mathrm{Sr})\mathrm{TiO}_3$ (BST) being the most explored ferroelectric materials for antenna applications [15], [16]. However, the lack of post-CMOS compatibility of these materials significantly hinders their large-scale manufacturability. Hafnium Zirconium Oxide (HZO), on the other hand, is a ferroelectric material already available in several CMOS foundries, showing a significant ferroelectric remnant polarization [17] when its thickness is within a few tens of nanometers [18].

In this work, we report a programmable on-chip monopole antenna whose resonance frequency can be tuned by leveraging the ferroelectric switching of the embedded HZO thin film. The device, fabricated on a Si/SiO_2 substrate through a fully CMOS compatible microfabrication process, exhibits an HZO metal-ferroelectric-metal (MFM) capacitor monolithically integrated into the antenna's microstrip feed line. The embedded HZO film enables non-volatile programmability of the antenna's response through its ferroelectric behavior, which is macroscopically evidenced by a variation of its relative permittivity [19].

Owing to the non-volatile properties of the ferroelectric film, the antenna shows frequency retention even after removing the DC source. Based on our findings, this is the first time that such behavior is reported for a ferroelectric-based programmable system. Furthermore, to the extent of our knowledge, this work shows the first example of ferroelectrically tunable millimeter wave (mmWave) antenna, marking the highest frequency ever reported for a similar devices. Given HZO's ultrafast switching speed [20], its relatively low

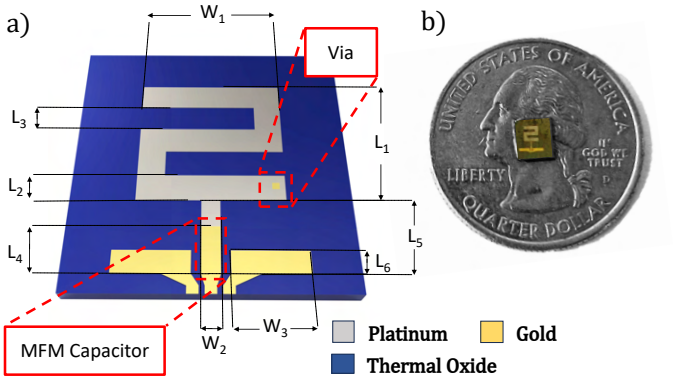

Fig. 1. a) Model of the proposed on-chip programmable meander-line monopole antenna. The via and the HZO MFM capacitor section, formed by the Pt-HZO-Au junction along the feed line, are highlighted in red. b) Fabricated programmable antenna in comparison to a U.S. quarter dollar.

TABLE I
IN-PLANE DIMENSIONS OF THE FERROELECTRICALLY-PROGRAMMABLE MEANDER-LINE MONOPOLE ANTENNA

Symbol	L_1	W_1	L_2	L_3	L_4	W_2	L_5	L_6	W_3
Length [μm]	1680	1500	360	300	458	115	1080	300	950

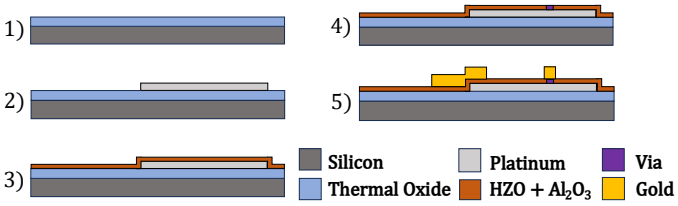

Fig. 2. Fabrication process and 5) cross-section of the proposed on-chip programmable antenna. A thermal oxide-coated Si wafer was used as a substrate for the sputter deposition of a patterned 100 nm-thick Pt bottom electrode. 20 nm-thick HZO was then grown via ALD, and subsequently etched to achieve direct electrical contact with the bottom electrode. Finally, a 200 nm-thick Au top electrode was deposited through e-beam evaporation.

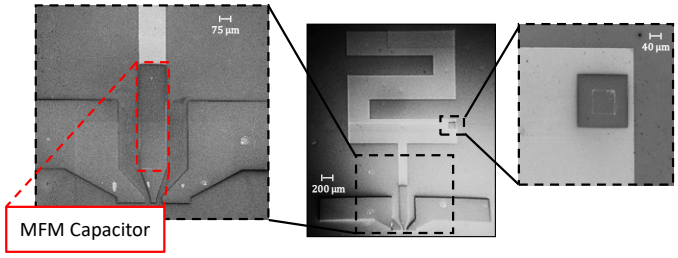

Fig. 3. SEM picture of the meander-line antenna, with emphasis on the monolithically-integrated HZO MFM capacitor structure along the microstrip line (left) and on the via structure (right).

programming voltage, its CMOS compatibility, and its ability to retain dielectric properties without a continuous bias, the reported device paves a new path towards adaptive CMOS compatible antennas for next-generation RFFEs.

II. DESIGN AND FABRICATION

The proposed antenna (Fig. 1), whose dimensions are shown in Table I, consists of a rectangular 2-shaped meander-line monopole [21] with overall dimensions of 1.68 mm in length (L_1) and 1.5 mm in width (W_1). The width of the meandered pattern is 360 μm (L_2), while the gaps are set to 300 μm (L_3). The meandered structure allows for the miniaturization of the antenna while maintaining the desired electrical length [22]. The antenna is composed of a patterned 100 nm-thick platinum (Pt) bottom electrode forming the meandered structure, in conjunction with a 20 nm-thick HZO layer and a 200 nm-thick gold (Au) top electrode. The HZO layer exhibits a relative dielectric permittivity ϵ_r of 25 and a dielectric loss tangent ($\tan\delta$) of 0.06 when no programming voltage is applied [19]. The antenna is built on top of a 100 mm high resistivity silicon (Si) substrate, coated with a 300 nm-thick thermal silicon dioxide (SiO_2).

A 1080 μm long (L_5) and 120 μm wide (W_2) 50 Ω coplanar waveguide (CPW)-to-microstrip transmission line is implemented to feed the antenna. The total electrical length of the radiating structure and its microstrip feed line is designed to be roughly 1/4 of the wavelength of operation. In this regard, the embedded HZO film allows fine-tuning of the effective electrical length of the monopole, resulting in a shift of the antenna's resonance frequency. Moreover, in order to maximize the programming effect of the embedded HZO layer, the location of the HZO MFM capacitor was chosen in accordance with the electric field distribution on the antenna. The structure was therefore placed in the lower end of the antenna's feed line, as per finite element analysis (FEA) simulations the electric field is maximized in that region. The in-plane dimensions of the HZO MFM structure (L_4 long and W_2 wide), coinciding with the size of the overlap between gold and platinum layers, are key design parameters for the reported antenna. Since W_2 was chosen in accordance with the size of the available on-chip probes, L_4 was the only parameter we could optimize to ensure proper matching conditions. In this regard, L_4 was chosen to ensure proper matching to 50 Ω when no DC voltage is applied.

Through our optimization process, we found that an L_4 of 458 μm ensured a good impedance matching in the mmWave frequency range. We also included a 45 μm by 45 μm via to ensure electrical access to the bottom metal plate and allow the ferroelectric polarization of the HZO film through DC probes.

The fabrication process of the proposed device is shown in Fig. 2 [23] and adopts CMOS-compatible microfabrication techniques. A 10 nm-thick titanium (Ti) layer was sputtered on the Si wafer for adhesion purposes. Afterwards, the 100 nm-thick meandered Pt bottom electrode was deposited through radio frequency (RF) sputtering. A bi-layer lift-off process was optimized to minimize fencing effects along the bottom electrode's edges.

A 20 nm-thick ferroelectric HZO layer and a 3 nm-thick Al_2O_3 capping layer were subsequently deposited through ALD. The thin HZO layer was grown by alternating pulses of tetrakis(dimethylamido)hafnium (TDMAHf) and

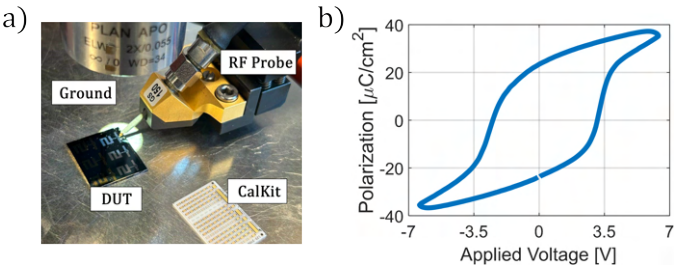

Fig. 4. a) Measurement setup for the proposed meander-line monopole antenna. b) Experimental ferroelectric polarization (P-E) loop of the deposited HZO film. The P-E loop was measured with a triangular waveform at 5 kHz through the Sawyer-Tower method.

tetrakis(dimethylamido)zirconium (TDMAZr) as precursors, each followed by water pulses as an O_2 source. The Al_2O_3 layer was instead deposited using alternating pulses of trimethylaluminum (TMA) and water. A via was then etched in the HZO film through an inductively-coupled plasma (ICP) fluorine etch. Subsequently, a 200 nm-thick Au top electrode was deposited through e-beam evaporation. Finally, the chip hosting the fabricated device was annealed through a rapid thermal annealing (RTA) processing step under N_2 for 60 s at a temperature of 450 °C. A scanning electron microscope (SEM) picture of the fabricated device is reported in Fig. 3.

III. Measurements and Discussion

The performance of the fabricated device was characterized through direct wafer probing, using a ground-signal-ground (GSG) probe with a 150 μm pitch (Fig. 4a). The S_{11} parameters were recorded using a Keysight N5221A vector network analyzer (VNA). First, we proceeded with the ferroelectric characterization of the HZO film. We extracted the polarization vs. applied DC voltage at 5 kHz (Fig. 4b) by using the Sawyer-Tower method on an AixACCT TF3000 Frequency Analyzer. We found a remnant polarization (P_r) of 24 μC/cm^2, in line with previous P_r values found for similar 20 nm-thick HZO films [18].

Later, we studied the effect of the HZO ferroelectric polarization on the antenna's resonance frequency by applying a partial polarization signal ranging between -5 V and +5 V in steps of 0.5 V. The electrical response of the antenna was measured after executing each voltage step and following the removal of the DC source. Our measurements (Fig. 5) highlight a ferroelectrically-induced programmability in the antenna's resonance frequency, justifying the occurrence of a hysteresis behavior in the antenna's resonance frequency vs. DC voltage profile. It is worth emphasizing that the non-volatile programmability of HZO allows us to record the shift of the resonance frequency of the antenna even without the continuous application of a DC bias. In fact, the embedded HZO film requires only a single voltage pulse to achieve ferroelectric switching.

Fig. 5 highlights the two operational points (A and B) showcasing the highest difference in resonance frequency and

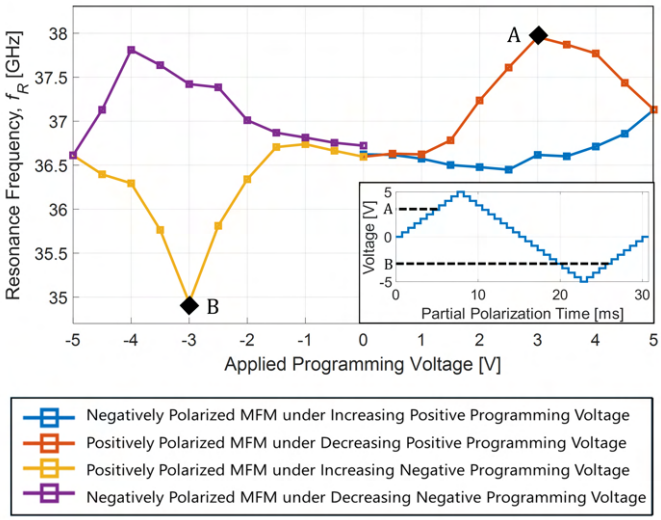

Fig. 5. Ferroelectrically-induced hysteresis loop of the antenna's resonance frequency in response to the applied programming voltage. Operational Point A denotes the maximum resonance frequency (37.957 GHz) obtained when applying a programming voltage of 3 V. Operational Point B marks the minimum resonance frequency (34.938 GHz) observed with a programming voltage of -3 V. The inset reports the applied voltage profile during the partial polarization experiment between -5 V and 5 V.

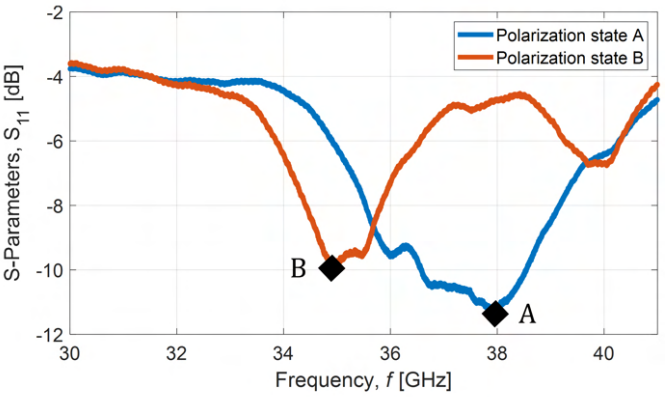

Fig. 6. Measured and simulated S_{11} parameters for Operational Point A (3 V) and Operational Point B (-3 V). Programming Voltages A and B mark the maximum ferroelectrically-induced frequency shift derived from the partial polarization experiment (see inset in Fig. 5). This shift is obtained by modifying the polarization states of HZO's domains.

the corresponding programming voltages (3 V and -3 V). We report the antenna's S_{11} vs. frequency trends for such points in Fig. 6. These trends were extracted after applying a single DC voltage pulse of 3 V for point A and -3 V for point B. After each set of measurements, we removed the DC source and measured the antenna's maximum resonance frequency shift without applying a continuous DC bias.

Evidently, the reported antenna shows resonance frequencies of 37.957 GHz and 34.938 GHz at points A and B, respectively. The measured frequency shift between the two points is 3.019 GHz, corresponding to a fractional frequency change (FFC) of 8.3%. Such change, computed between the

TABLE II
COMPARISON BETWEEN DIFFERENT FERROELECTRIC-BASED THIN FILM RECONFIGURABLE ANTENNAS

Work	Frequency Range†	Material	Area	CMOS Compatibility	Monolithically Integrated	Voltage	Fractional Frequency Change	Non-Volatile Programmability
[13]	17–17.3 GHz	KTN	100 mm^2	No	Yes	0–150 V	1.7%	No
[14]	15.2–16 GHz	KNN	16 mm^2	No	Yes	0–150 V	4.6%	No
[15]	0.6–0.75 GHz	BST	645 mm^2	No	Yes	0–30 V	14.5%	No
[16]††	28–30.7 GHz	BST	1.75 mm^2	No	Yes	0–100 V	16.7%	No
[17]	9–9.2 GHz	HZO, Metamaterial, Resonator	139.7 mm^2	Yes	No	±2 V	Not Provided, 1.8% Estimated	No
This work	34.9–37.9 GHz	HZO	6.5 mm^2	Yes	Yes	±5 V	8.3%	Yes

†Measured resonance frequencies at the maximum frequency variation.
††The results of this work are only based on simulations, no physical device was built.

lowest (RF_B) and the highest (RF_A) experimentally measured resonance frequencies at different applied voltages, was determined as reported in [14]:

$$\mathrm{FFC} = \left| \frac{\mathrm{RF}_B - \mathrm{RF}_A}{(\mathrm{RF}_B + \mathrm{RF}_A)/2} \right| \times 100 \tag{1}$$

A comparison between this work and other ferroelectric-based reconfigurable antennas is presented in Table II. The reported HZO-based antenna shows a smaller area and requires a significantly lower voltage to achieve ferroelectric switching compared to most demonstrated counterparts. Together with the overall CMOS compatibility and low power consumption, the non-volatile programmability of the presented HZO-based device offers strong advantages over the BST, KNN, and KTN counterparts.

Such a feature enables our antenna to retain its programmed resonance frequency value without having to continuously apply a bias, since the embedded HZO film can achieve ferroelectric switching even with a single DC pulse. Furthermore, the lack of a continuous bias allows for the relaxation of the design constraints of electrostatic discharge protection circuits [24]. Compared to another HZO-based device reported in the literature [17], this design exhibits a more compact form factor (area of only 6.5 mm^2), non-volatile programmability of the resonance frequency, and a fractional frequency change of 8.3%, which is more than four times the one found in [17].

IV. CONCLUSION

In this work, a ferroelectrically programmable mmWave on-chip monopole antenna is presented. Owing to the ferroelectric properties of the nanometers-thick HZO film, the reported antenna shows significant ferroelectric programmability, resulting in a 8.3% fractional shift of its resonance frequency without having to continuously apply DC voltages. This marks, based on our findings, the first example of a bias-less ferroelectrically programmable antenna. To the best of our knowledge, this work is the first demonstration of a fully mmWave ferroelectric-based programmable antenna, marking the highest operational frequency ever reported for such devices. The combination of the compact size, full CMOS compatibility, non-volatile programmability, and low programming voltage marks a substantial advancement over state-of-the-art devices in this field. This frames the proposed HZO-based programmable antenna as a promising candidate for future 5G and 6G-grade chip-scale transceivers.

REFERENCES

[1] I. F. Akyildiz, A. Kak, and S. Nie, "6G and beyond: The future of wireless communications systems," *IEEE Access*, vol. 8, pp. 133995–134030, 2020.

[2] R. L. Haupt and M. Lanagan, "Reconfigurable antennas," *IEEE Antennas and Propagation Magazine*, vol. 55, no. 1, pp. 49–61, 2013.

[3] S. Park, J.-L. Woo, U. Kim, and Y. Kwon, "Broadband CMOS stacked RF power amplifier using reconfigurable interstage network for wideband envelope tracking," *IEEE Transactions on Microwave Theory and Techniques*, vol. 63, no. 4, pp. 1174–1185, 2015.

[4] O. P. Kumar, P. Kumar, T. Ali, P. Kumar, and S. Vincent, "Ultrawideband antennas: Growth and evolution," *Micromachines*, vol. 13, no. 1, 2022.

[5] E. Erdil, K. Topalli, M. Unlu, O. A. Civi, and T. Akin, "Frequency tunable microstrip patch antenna using RF MEMS technology," *IEEE Transactions on Antennas and Propagation*, vol. 55, no. 4, pp. 1193–1196, 2007.

[6] M. Dragoman, D. Neculoiu, A.-C. Bunea, G. Deligeorgis, M. Aldrigo, D. Vasilache, A. Dinescu, G. Konstantinidis, D. Mencarelli, L. Pierantoni, and M. Modreanu, "A tunable microwave slot antenna based on graphene," *Applied Physics Letters*, vol. 106, p. 153101, 04 2015.

[7] A.-K. U. Michel, D. N. Chigrin, T. W. W. Maß, K. Schönauer, M. Salinga, M. Wuttig, and T. Taubner, "Using low-loss phase-change materials for mid-infrared antenna resonance tuning," *Nano Letters*, vol. 13, no. 8, pp. 3470–3475, 2013. PMID: 23742151.

[8] F. Bayatpur and K. Sarabandi, "A tunable metamaterial frequency-selective surface with variable modes of operation," *IEEE Transactions on Microwave Theory and Techniques*, vol. 57, no. 6, pp. 1433–1438, 2009.

[9] A. Ahmed, I. A. Goldthorpe, and A. K. Khandani, "Electrically tunable materials for microwave applications," *Applied Physics Reviews*, vol. 2, p. 011302, 02 2015.

[10] N. Setter, D. Damjanovic, L. Eng, G. Fox, S. Gevorgian, S. Hong, A. Kingon, H. Kohlstedt, N. Y. Park, G. B. Stephenson, I. Stolitchnov, A. K. Taganstev, D. V. Taylor, T. Yamada, and S. Streiffer, "Ferroelectric thin films: Review of materials, properties, and applications," *Journal of Applied Physics*, vol. 100, p. 051606, 09 2006.
[11] H. Jiang, M. Patterson, C. Zhang, and G. Subramanyam, "Frequency tunable microstrip patch antenna using ferroelectric thin film varactor," in *Proceedings of the IEEE 2009 National Aerospace & Electronics Conference (NAECON)*, pp. 248–250, 2009.
[12] S. Courrèges, Z. Zhao, K. Choi, A. Hunt, and J. Papapolymerou, "Electronically tunable ferroelectric devices for microwave applications," in *Microwave and millimeter wave technologies from photonic bandgap devices to antenna and applications*, IntechOpen, 2010.
[13] F. Cissé, *Dispositifs hyperfréquences et antennes périodiques reconfigurables à base de films minces ferroélectriques des systèmes KTN-KNN*. PhD thesis, Rennes 1, 2017.
[14] B. Aspe, X. Castel, V. Demange, S. Députier, V. Bouquet, R. Benzerga, R. Sauleau, and M. Guilloux-Viry, "Frequency-tunable slot-loop antenna based on KNN ferroelectric interdigitated varactors," *IEEE Antennas and Wireless Propagation Letters*, vol. 20, no. 8, pp. 1414–1418, 2021.
[15] H. V. Nguyen, R. Benzerga, C. Borderon, C. Delaveaud, A. Sharaiha, R. Renoud, C. L. Paven, S. Pavy, K. Nadaud, and H. W. Gundel, "Miniaturized and reconfigurable notch antenna based on a BST ferroelectric thin film," *Materials Research Bulletin*, vol. 67, pp. 255–260, 2015.
[16] V. Muzzupapa, A. Crunteanu, D. Passerieux, C. Borderon, R. Renoud, H. W. Gundel, and L. Huitema, "Frequency reconfigurable millimeter wave antenna integrating ferroelectric interdigitated capacitors," in *2023 17th European Conference on Antennas and Propagation (EuCAP)*, pp. 1–4, 2023.
[17] M. Aldrigo, A. C. Tasolamprou, D. Vasilache, M. Kafesaki, S. Iordanescu, F. Nastase, and M. Dragoman, "Tunable microwave dual-band patch antenna through integration of metamaterials and nanoscale ferroelectrics," *Phys. Rev. Appl.*, vol. 20, p. 044067, Oct 2023.
[18] N. Casilli, O. Kaya, T. Kaisar, B. Davaji, P. X.-L. Feng, and C. Cassella, "Nonvolatile state configuration of nano-watt parametric ISING spins through ferroelectric hafnium zirconium oxide MEMS varactors," in *2023 IEEE 36th International Conference on Micro Electro Mechanical Systems (MEMS)*, pp. 511–514, 2023.
[19] S. Abdulazhanov, Q. H. Le, D. K. Huynh, D. Wang, D. Lehninger, T. Kämpfe, and G. Gerlach, "THz thin film varactor based on integrated ferroelectric HfZrO2," *ACS Applied Electronic Materials*, vol. 5, no. 1, pp. 189–195, 2023.
[20] M. Si, X. Lyu, P. R. Shrestha, X. Sun, H. Wang, K. P. Cheung, and P. D. Ye, "Ultrafast measurements of polarization switching dynamics on ferroelectric and anti-ferroelectric hafnium zirconium oxide," *Applied Physics Letters*, vol. 115, p. 072107, 08 2019.
[21] Z. Konstas, A. Rida, R. Vyas, K. Katsibas, N. Uzunoglu, and M. M. Tentzeris, "A novel "green" inkjet-printed Z-shaped monopole antenna for RFID applications," in *2009 3rd European Conference on Antennas and Propagation*, pp. 2340–2343, 2009.
[22] O. P. N. Calla, A. Singh, A. Kumar Singh, S. Kumar, and T. Kumar, "Empirical relation for designing the meander line antenna," in *2008 International Conference on Recent Advances in Microwave Theory and Applications*, pp. 695–697, 2008.
[23] O. Kaya, L. Colombo, B. Davaji, and C. Cassella, "A non-volatile threshold sensing system using a ferroelectric Hf0.5Zr0.5O2 device and a LiNbO3 microacoustic resonator," in *2023 IEEE 36th International Conference on Micro Electro Mechanical Systems (MEMS)*, pp. 161–164, 2023.
[24] S. H. Voldman, *ESD: circuits and devices*. John Wiley & Sons, 2015.